analytical chemistry

ARTICLE

pubs.acs.org/ac

Carcinoembryonic Antigen Admittance Biosensor Based on Au and ZnO Nanoparticles Using FFT Admittance Voltammetry

Parviz Norouzi,[*,†,‡] Vinod Kumar Gupta,[§,⊥] Farnoush Faridbod,[‡] Morteza Pirali-Hamedani,[∥,#] Bagher Larijani,[‡] and Mohammad Reza Ganjali[†,‡]

[†]Center of Excellence in Electrochemistry, University of Tehran, Tehran, Iran

[‡]Endocrinology & Metabolism Research Center, Tehran University of Medical Sciences, Tehran, Iran

[§]Department of Chemistry, Indian Institute of Technology, Roorkee 247667, India

[⊥]Chemistry Department, King Fahd University of Petroleum & Minerals, Dhahran 31261, Saudi Arabia

[∥]Department of Medical Chemistry, Faculty of Pharmacy, Tehran University of Medical Sciences, Tehran, Iran

[#]Pharmaceutical Sciences Research Center, Tehran, Iran

ABSTRACT: In this work, a highly sensitive carcinoembryonic antigen fast Fourier transform admittance biosensor is introduced. The proposed biosensor is based on bilayer films of ZnO/Au nanoparticles as an immobilization matrix. These layers are prepared by self-assembly and deposition method on a gold electrode surface, respectively. Carcinoembryonic antibody (anti-CEA) was immobilized on gold nanoparticles and positively charged horseradish peroxidase (HRP) was used to block sites against nonspecific binding. The admittance biosensor was developed based on fast Fourier transform continuous square wave voltammetry, which produces a sensitive, fast (less than 20 s) and reliable response for determination of carcinoembryonic antigen. The technique was applied as a detector in a flow injection system. The admittances reduction current of the biosensor decreases linearly in two concentrations ranges of CEA from 0.1 to 70 ng/mL and from 70 to 200 ng/mL with a detection limit of 0.01 ng/mL in presence of 0.5 mM H_2O_2 as an eluent solution.

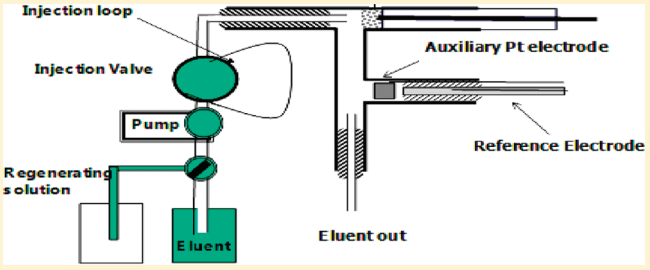

The carcinoembryonic antigen (CEA) is a glycoprotein that is normally produced during the development of a fetus. The production of CEA stops before birth, and it usually is not present in the blood of healthy adults. However, this protein may appear in the blood of some people who have certain kinds of cancers, especially large intestine (colon and rectal) cancer. Also CEA may be present in people who have cancer of the pancreas, breast, ovary, or lung. The carcinoembryonic antigen (CEA) level shows that how cancer is widespread and after treatment or surgery shows the success of treatment or chances of recovery. Thus, CEA can be a good cancer biomarker.[1,2]

Development of numerous immunochemical methods for the measurement of antigen−antibody reactions is the interest subject of several researches.[3−6] Recently, electrochemical methods find important roles due to their simple pretreatment procedure, fast analytical response time, precise and sensitive current measurement, inexpensive and miniaturizable instrumentation.[7−14] However, most of amperometric immunoassay techniques are based on the amplification of enzyme-label of either antigen or antibody, which requires highly qualified operators, tedious assay time, or sophisticated instrument.

Literature survey reveals that there are some reports on electrochemical based immuno-sensors for carciembryonic antigen detection.[15−26] Some of them will be compared to proposed techniques at the end of this article.

During recent years, nanoparticles have been widely used in construction of electrochemical biosensors.[27,28] One of the interesting metal oxide nanoparticles which has an interesting properties for using in electrochemical biosensors is ZnO nanoparticles (ZnO-NPs). ZnO-NPs has a high isoelectric point, which is about 9.5.[28] In biological pH, which is lower than its isoelectric points, the surface of ZnO metal oxide nanoparticle has a positive charge. Thus, protein with low isoelectric point (in case of CEA is 4.7) can be immobilized on it by an electrostatic force.[29,30] In addition, ZnO-NPs shows nontoxicity, good biocompatibility and high chemical stability when it used in construction of biosensors.[28]

The unique properties of gold nanoparticles (AuNPs), such as providing a suitable microenvironment for enzymes to immobilize but keep their biological activity, and facilitating electron transfer between the immobilized enzyme and electrode surfaces, have led to a wide use of this nanomaterial in construction of electrochemical biosensors.[31]

Received: August 28, 2010
Accepted: January 8, 2011
Published: February 10, 2011

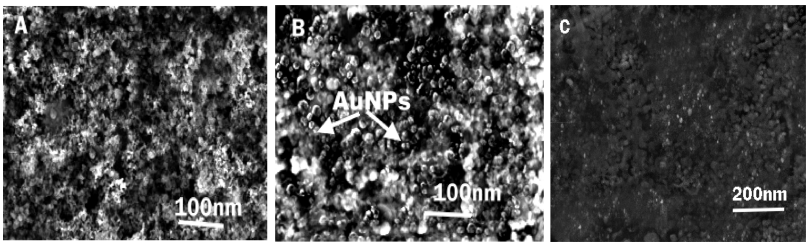

Figure 1. SEM images of: (A) the electrode surface modified by ZnO NPS, (B) Au nanoparticles deposited on the electrode surface, and (C) the electrode surface coated by the antibody.

In this work, horseradish peroxidase (HRP) is used on bilayer films of the electrode as a blocking agent to block possible remaining active sites of the AuNPs monolayer and amplify the response of the antigen−antibody reaction at the same time.

The detection method, fast Fourier transform square wave voltammetry (FFTSWV), which is used here, is very sensitive, inexpensive, and fast. The square wave voltammetry (SWV) has recently been shown to be advantageous for environmental detection of several compounds.[32−34] This paper describes a fundamentally different approach to SWV measurement, in which the detection limits are improved, while preserving the information content of the SW voltammogram. In fact, the analyte signal is calculated based on admittance changes related to the changes in electrical double layer.

Using fast Fourier transform method in combination with electrochemical method provide a sensitive technique for trace detection of compounds.[12,13,35−37] In particular, when the magnitude of the current is in the range of nano and pico ampere, electrochemical response suffers from existence of environmental noises. The approach used here is designed to separate the voltammetric signal and background signal in frequency domain by using discrete fast Fourier transformation (FFT) method. This separation allows, digitally filtrating some of the noises and decreasing the bandwidth of the measurement. Furthermore, improvement in the signal was gained by two-dimensional integration of the electrode response over a selected potential range and time window of the signal.

MATERIALS AND METHODS

Reagents. All chemicals and solvents used were of analytical grade and used as received. Double distilled water was used throughout the experiments. ZnO nanoparticle, 99%, 20 nm, specific surface area 90 m^2/g was purchased from local Company (Nanopars). Horseradish peroxidase (HRP, EC 1.11.1.7, RZ > 3.0, A > 250 U/mg), $HAuCl_4$ were obtained from Sigma. Carcinoembryonic Antigen from human fluids and Monoclonal Anti-Carcinoembryonic Antigen antibody produced in mouse were purchased from Aldrich. The prepared solutions were kept at 4 °C before use. Gold nanoparticles were produced by reducing $HAuCl_4$ on the electrode surface. The mean size of the prepared Au colloids was about 15 nm, estimated by transmission electron microscopy. The solution of 3 mM $Fe(CN)_6^{4-}/^{3-}$ in 0.02 M PBS was used as an electrochemical probe for studying the modification of the electrode surface. The CEA was frozen, and its standard solutions were prepared daily with double distilled water when in use.

Instrumentation. The electrochemical instrument, for voltammetric measurements, was a homemade potentiostat. The potentiostat was connected to a PC PIV equipped with a data acquisition board (PCL-818H, Advantech Co.), which was used to output an analog waveform and acquire current readings. The memory and CPU requirements of the computer were dictated by the nature of the data acquisition requirements. Software was developed using Delphi 6.0 to apply repeatedly a waveform to the working electrode and synchronously acquire, analyze, and store the current data. The controlling program was accompanying dynamic link libraries allowed waveform generation and current sampling to be synchronized, which was essential in interpreting SWV current response. The data could be interpreted and plotted in real time or stored data could be loaded and reanalyzed to generate voltammogram. Most of the waveform parameters could be modified within the software; including the pre and post scan potential/time, square wave frequency/amplitude, dc ramp initial/final potential, and ramp time.

Biosensor Electrode Preparation. The surface of an Au disk electrode (d = 3 mm) was polished well with 0.3 μm alumina slurry. After the electrode was rinsed with doubly distilled water, the electrode was successively sonicated in solution of 1:1 nitric acid and ethanol. Next for final cleaning, the electrode was transferred into the solution of 0.1 M H_2SO_4 by continuous cyclic voltammetry method cyclized between −0.4 and +1.5 V versus SCE at 1 V/s until a stable cyclic voltammogram was obtained. After the electrode was rinsed with doubly distilled water, 20 μL of ZnO-nanoparticles (5%; pH 2.0−3.0) was dropped onto the electrode surface and was dried in the air. Electrostatic force is the driving force for sticking ZnO nanoparticles on the gold electrode surface. The iso-electric point of ZnO nanoparticle is about 9.5. In acidic pH, which is lower than its iso-electric pH, the surfaces of the nanoparticles have a positive charge. While the surface of Au electrode has a potential of zero charge about −0.2 V, thus, an electrostatic force causes ZnO nanopraticles stick on the gold electrode surface.

The electrochemical deposition of AuNPs was performed in 0.2 M Na_2SO_4 aqueous solution of $HAuCl_4$ (1.0 mM). The deposition time was about 200 s and the potential was −0.2 V. The electrode was then washed with doubly distilled water carefully, and it was immersed in 0.5 mL anti-CEA solution at 4 °C for about 12 h. Finally the proposed electrode was incubated in HRP solution for about 4 h at 4 °C for block remaining active sites of the AuNPs monolayer and amplifies the response of the antigen−antibody reaction. Scanning electron microscopic (SEM) images of electrode surface modification were shown in Figure 1. Also, the schematic diagram of the stepwise procedure of the biosensor preparation was shown in Figure 2a. The biosensor was stored at 4 °C.

Flow Injection Setup. For flow injection measurements, the system included an 8 rollers peristaltic pump (Ultratech. Laboratories Co., Iran) and a four ways injection valve (Supelco Rheodyne Model 5020) with a 700 μL sample injection loop.

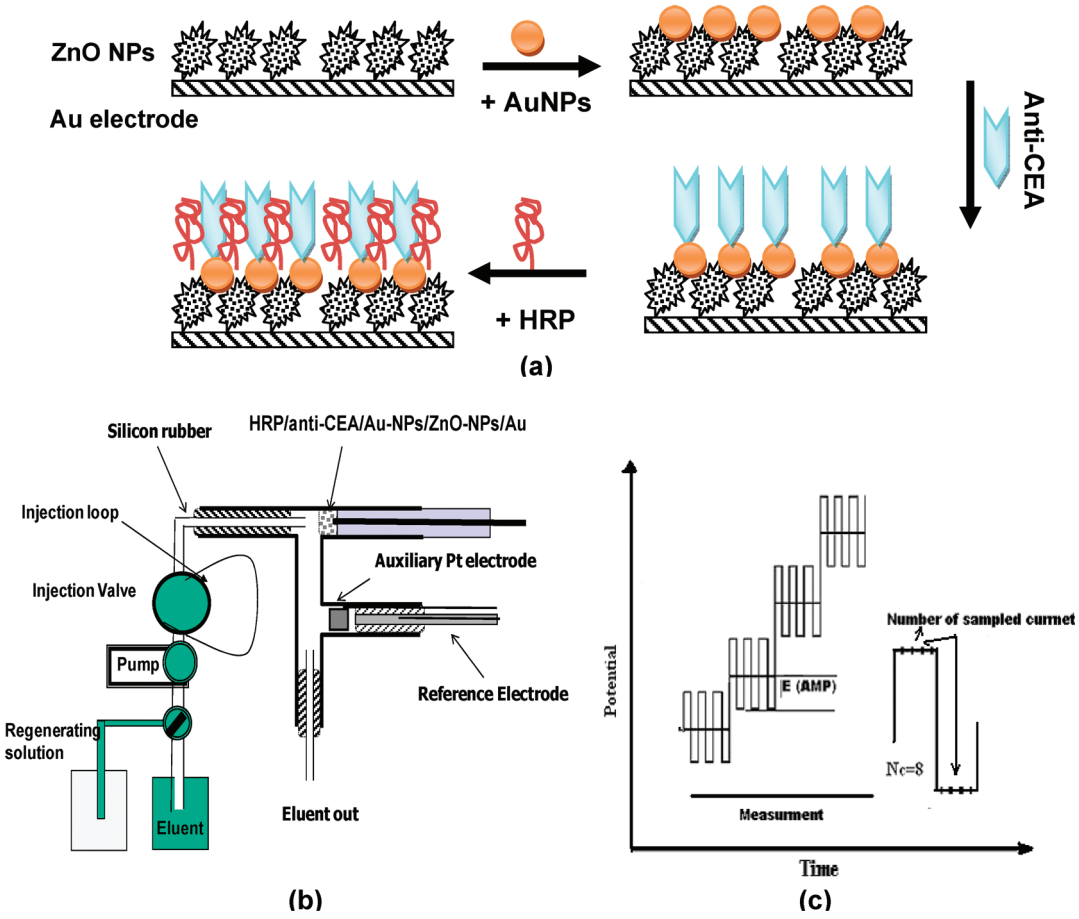

Figure 2. (a) Schematic figures of electrode surface preparation. (b) Electrochemical cell used in flow injection analysis. (c) Diagram of potential waveform used for FFTSW voltammetry.

Solutions were introduced into the sample loop by using of a 1 mL plastic syringe. The electrochemical cell used in flow injection analysis is shown in Figure 2b.

Square Wave Voltammetry. The analyte measurements were carried out in the continuous fast Fourier transform square wave (FFTSW) voltammetric mode. In this method to improve the sensitivity of the analytes response, the applied SW potential waveform, current sampling and data processing was modified. The modified potential waveform is shown in Figure 2c. As it is shown, the measurement part of the waveform contains multiple SW pulses with amplitude of E_{sw} and frequency of f_o, were superimposed on a staircase potential function, which was changed by a small potential step of ΔE (10 mV). The values of potential pulse of SW ($E_{(amp)}$) was in the range of 5−35 mV. In potential ramp, the currents were sampled four times per each SW polarization cycle.

RESULTS AND DISCUSSION

Electrochemical impedance spectroscopy (EIS) used to characterize the sequence of assembly of the materials in biosensor. A three millimolar solution of $Fe(CN)_6^{4-/3-}$ was used for as a redox probe, and the results are shown in Figure 3. The curves are the results of Faradic EIS of bare Au electrode (curve a), ZnONPs/Au electrode (curve b), Au-NPs/ZnO-NPs/Au electrode (curve c), and HRP/anti-CEA/Au-NPs/ZnO-NPs/Au electrode (curve d) in the presence of $Fe(CN)_6^{4-/3-}$ as a redox probe. It can be seen that when the surface of the bare Au electrode (curve a) was coated with ZnO-NPs, the impedance of the electrode surface increased, which is due to the difficulty of charge transfer on ZnO-NPs film. But addition of conductive Au-NPs layer decreases the total electrode impedance. Finally, when the HRP/anti-CEA were absorbed on the surface of Au-NPs/ZnO-NPs/Au electrode, both Z_{img} and Z_{rel} increase (curve d), which indicates anti-CEA is strongly bound to the electrode surface.

Figure 4 shows FFTSW voltammograms and the changes in admittance of the HRP/anti-CEA/AuNPs/ZnONPs/Au electrode in the solution of 0.02 M PBS (pH = 5.9), 3 mM $Fe(CN)_6^{4-/3-}$ and 0.5 mM H_2O_2. In this measurement, the FFTSW pulse had amplitude of 25 mV and a frequency of 350 Hz in the potential range from −200 to 800 mV. The figure shows that before injection (in absent of CEA) there is no significant changes in the voltammograms but, by injection of 700 μL of 5 ng/mL CEA in 0.02 M PBS at pH = 5.9, a signal appears about potential of 320 mV.

Decrease in the admittance of the electrode is proportional to the CEA concentration in two ranges from 0.1 to 70 ng/mL and from 70 to 200 ng/mL when 1 mg/mL HRP is used as blocking agent. The HRP immobilized on nano-Au monolayer performed an effective amplification of the current signal and improve the sensitivity of the immunosensor.

The results show that by increasing the concentration of CEA in the injected sample the admittance decreases and 96% of steady state response is achieved in less than 20 s, which confirms a good electrocatalytic and fast electron exchange behavior of modified electrode.

dx.doi.org/10.1021/ac102270w |*Anal. Chem.* 2011, 83, 1564–1570

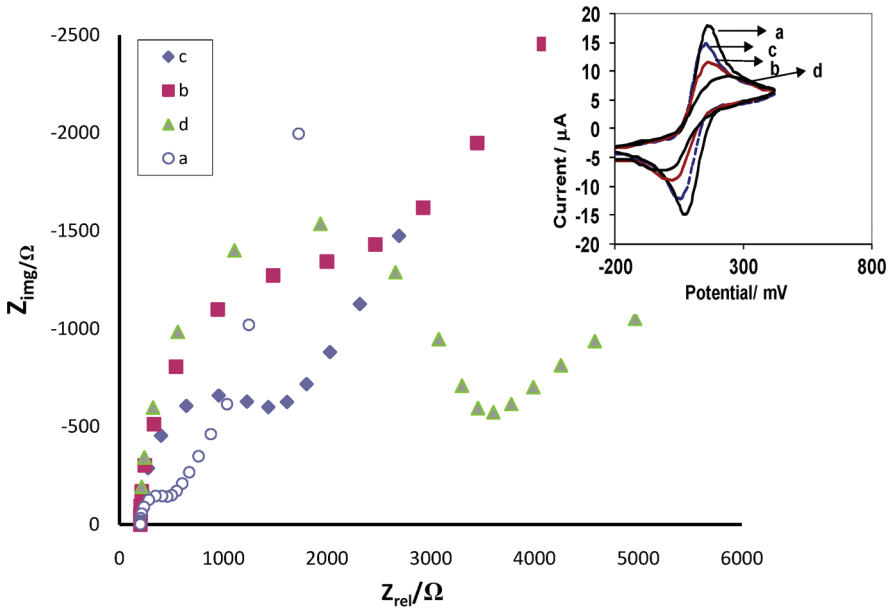

Figure 3. EIS of (a) bare Au electrode, (b) ZnO-NPs/Au electrode, (c) Au-NPs/ZnO-NPs/Au electrode, and (d) HRP/anti-CEA/Au NPs/ZnO-NPs/Au electrode in the solution of 0.02 M PBS (pH = 5.9) and 3 mM $Fe(CN)_6^{4-/3-}$. Inset: Cyclic voltammograms of different stages obtained in scan rate of 300 mV/s.

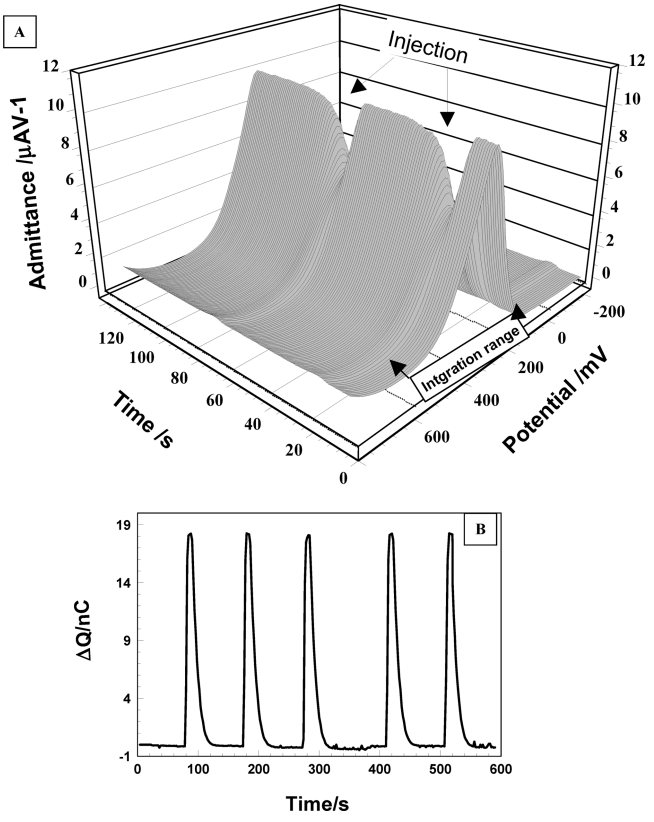

Figure 4. A: Admittance voltamograms of the HRP/anti-CEA/Au-NPs/ZnO-NPs/Au electrode in the solution of 0.02 M PBS (pH = 5.9) and 3 mM $Fe(CN)_6^{4-/3-}$ with 0.5 mM H_2O_2 without (in absent) and with injection of 5.0 ng/mL CEA in the potential range of −200 to 800 mV at frequency of 300 Hz and amplitude of 25 mV. B: Calculated response of the electrode for several injections of 5.0 ng/mL CEA.

The adsorption of the analytes onto the gold surface reported a detection method by using flowing systems cyclic voltammetry to monitor the adsorption of several inorganic and organic molecules onto Au electrode. Once FFTSWV is used to monitor a flowing system, CEA electrochemical processes will cause a measurable change in the admittance voltammogram. To overcome these drawbacks, a new amplification strategy was introduced for improving the sensitivity of immunosensor by means of immobilizing HRP in bilayer films and using it as blocking agent. The mechanism of the amplification strategy is as follows: the immobilized HRP displayed the enzymatic activity to the constant concentrations of H_2O_2, which resulted in the amplified current signal. With the formation of the anti-CEA and CEA biocomplex on the electrode surface, a more obvious decrease of response could be obtained because of the formed biocomplex came into a barrier for the electrons to shuttle between the redox center of HRP and gold electrode. And the possible mechanism of reaction of H_2O_2 catalyzed by HRP is exemplified by the following schemes:

$$HRP_{(Red)} + H_2O_2 \rightarrow HRP_{(Ox)} + H_2O$$

$$\text{ferricyanide}_{(Red)} + HRP_{(Ox)} \rightarrow HRP_{(Red)} + \text{ferricyanide}_{(Ox)}$$

$$\text{ferricyanide}_{(Ox)} + e^- \rightarrow \text{ferricyanide}_{(Red)}$$

HRP blocks possible remaining active sites on the nanoparticles and avoids the nonspecific adsorption; also its interaction with H_2O_2 amplifies the biosensor response. In absence of CEA, H_2O_2 interact with HRP, and the product then interact with ferricyanide to make a signal.

When the proposed immunosensor reacts with CEA solution, a decrease in the peak current (or admittance of the electrode) can be observed, which is due to the changes of the electrode surface circumstance after the immuno-reaction.[17,18] In fact, by adsorption of CEA on the electrode surface the active center of HPR may be inhibited by CEA, which lowered the high turnover rate of the enzymatic reaction and the interaction of H_2O_2 with HPR, thus, a decrease in signal occurs.

dx.doi.org/10.1021/ac102270w |*Anal. Chem.* 2011, 83, 1564–1570

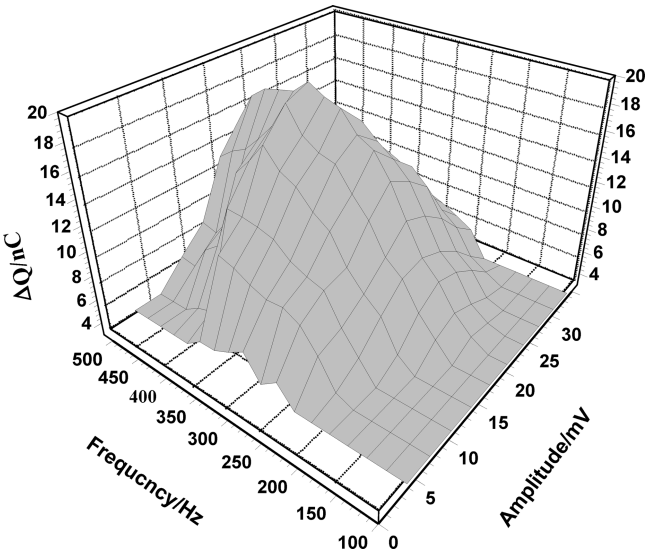

Figure 5. Effect of frequency and amplitude on the response of the modified electrode for 5.0 ng/mL CEA.

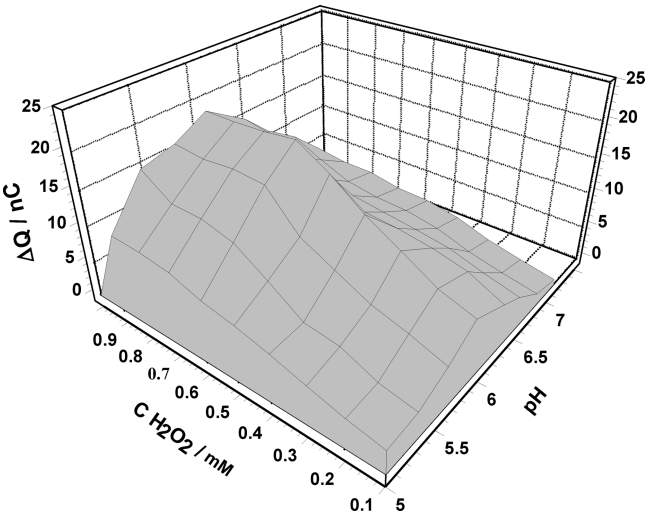

Figure 6. Effect of pH and H_2O_2 concentration on the response of modified electrode for 5.0 ng/mL CEA.

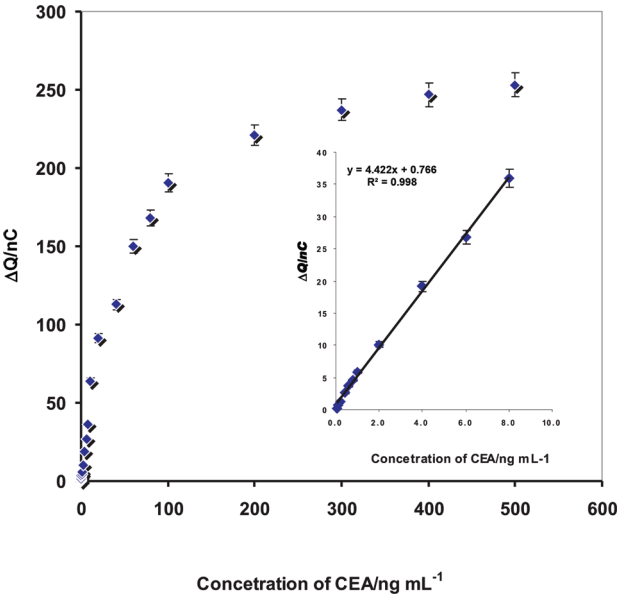

Figure 7. Calibration curves for CEA determination obtained by using HRP as blocking agents. The line shows a linear relationship between the peak reduction current and CEA concentration. In 0.02 M PBS (pH = 5.9); 3 mM $Fe(CN)_6^{4-/3-}$ with 0.5 mM H_2O_2. Error bars denote the relative standard deviation of triplicate measurements of each CEA concentration.

It is advantageous in FFTSWV to collect more current samples near the end of the forward and reverse pulses and use signal averaging to increase the S/N. It is well-known that in the traditional Osteryoung SWV method, the current is sampled at two points for each square wave, t_1 (the end of the first SW pulse) and t_2 (the end of the second SW pulse). In the Osteryoung technique, the majority of the charging current will have decayed at the end of each pulse, allowing the faradic current to be sampled independently. The FFTSWV is able to sample the current across the entire SW period and uses a selected section of the forward and reverse voltammogram for calculation of the difference in current. One of the advantages of scanning approaches for electrochemical detection is that all absolute changes in voltammogram can be selected for a calculation of the detector signal, based on response integration. A total absolute difference function ΔQ can be calculated by using the following equation:

$$\Delta Q(s\tau) = \Delta t\left[\sum_{E=E_i}^{E=E_v} |A(s, E).E - A(s_r,E).E|\right] \qquad (1)$$

Where s is the sweep number, τ is the time period between subsequent sweeps, Δt is the time difference between two subsequent points on the FFTSW curves, $A(s,E)$ represents the admittance of the FFTSW curve recorded during the sth sweep, and $A(s_r,E)$ is the reference admittance of the FFT-SW curve. E_i and E_v are the initial and the vertex potential, respectively. The reference FFTSW curve was obtained by averaging a few FFTSW curves (10−30) recorded at the beginning of the experiment (i.e., before injection of the CEA sample solution). By optimizing accumulation potential and time, the square-wave amplitude the ΔQ response can be maximized.

Optimization of FFTSW Frequency and Amplitude. In fast voltammetric analysis, the SW frequency and amplitude are important factors since the signal, background noise, and peak shape of CEA, depends on condition of excitation signal. To obtain the optimum SW waveform condition in for maximum ΔQ, the SW frequency range 100−500 Hz and amplitude 5−35 mV were examined. In Figure 5, the importance of frequency and amplitude is demonstrated for solution of 5 ng/mL CEA.

It should be noted that the solution resistance, electrode diameter, and stray capacitance of the system will limit the sensitivity gains obtained by raising the SW frequency. On the other hand, increasing the SW frequency and amplitude will increase the SW peak current of CEA, but this also will be enhanced by a higher charging/faradic current ratio.

It is well-known that the SW frequency and amplitude acts similar to sweep rate in cyclic voltammetry. In fact, using very high SW frequencies causes a shorter potential scan times, consequently, the response peak for the flow analysis becomes smaller and skewed, because of insufficient time for the electrochemical process of CEA on the electrode surface. While at lower

dx.doi.org/10.1021/ac102270w |*Anal. Chem.* 2011, 83, 1564–1570

Table 1. Comparison of the Proposed Biosensor with the Some Previous Reported Electrochemical Biosensors Based on Utilization of Different Materials and Methods

ref	detection method	DL	LR	materials
15	capacitance	10 pg/mL	0.01−10 ng/mL	self-assembled thiourea monolayer
16	voltammetry	0.1 ng/mL	0.5−20 ng/mL	glutathione (GSH) monolayer-AuNPs
17	amperometry	0.5 ng/mL	0.5−3 and 3−167 ng/mL	thionine and horseradish peroxidase-labled CEA
18	amperometry	0.9 ng/mL	2.5−80.0 ng/mL	AuNPs-thionine
24	amperometry	0.34 ng/mL	1−100 ng/mL	gold nanoparticles and SiO_2/Thionine nanocomposite
this work	admittance FFTCCV	0.01 ng/mL	0.1−70 ng/mL and 70 to 200 ng/mL	Au/ZnO NPs

SW frequencies which led to a longer potential scan times, result lower number of potential scan for each injected sample zone. This can cause a decline in ΔQ-time response. The results show that the optimal amplitude for the detection of CAE is 25 mV. In Figure 4 the plot of SW frequency versus ΔQ shows that frequency of 350 Hz was the optimal frequency.

Optimization of pH and H_2O_2 Concentration. Figure 6 shows the result of examination of H_2O_2 concentration and pH on the immunosensor sensitivity.

As mentioned above, since the amplifying performance of the immobilized HRP is H_2O_2 dependent, the amount of H_2O_2 concentration should be optimized. As seen in Figure 6, as the concentration of the H_2O_2 increases, the signal also increases until saturation occurs. This indicates that the HRP immobilized on the electrode surface retained in high enzymatic activity. The electrode response increases when the amounts of H_2O_2 were in the range of 0.1 to 0.6 mM. When H_2O_2 concentration was more than 0.5 mM (up to 1 mM), the electrode response tended to a constant value. Thus, 0.5 mM H_2O_2 was chosen for the measurement of CEA.

Moreover, the figure indicates that the electrode response increases with increasing pH up to 5.9, and by going to higher pHs decreases. Considering the facts that the enzyme can be denatured at higher pH and that the antibody−antigen complex may decompose of at lower pHs, pH 5.9 is used during the experiments.

Calibration Curve. Figure 7 illustrates a typical ΔQ response of the modified electrode on a standard solution of CEA (from 0.1 to 500.0 ng/mL in 0.02 M PBS solution (pH = 5.9). The experimental conditions were set at optimum values to obtain the best detection limits. Results shown in this figure represent the integrated signal for 3−5 consecutive flow injections of the standard solution. Under optimized conditions, the steady-state admittance showed two linear dynamic ranges of 0.1−70.0 and 70−200 ng/mL (Figure 7). A correlation coefficient of $R = 0.998$ with %RSD values ranging from 0.31−4.2% across the concentration range studied were obtained following linear regression analysis. As mentioned above the electrode response could be expressed in various ways as peak heights or peak areas. For this reason, the magnitude of the flow-injection peaks depends on the choice of the data processing methods. Measurements carried out for small analyte concentrations to allow the estimation of the detection limit C_{DL}

$$C_{DL} = \frac{3s_b}{\text{slope}} \qquad (2)$$

where s_b is the standard deviation (or noise) of the baseline around the flow-injection peak. The linearity was evaluated by linear regression analysis, which calculated by the least-squares regression method.

The LOD was measured as the lowest amount of the analyte that may be detected to produce a response, which is significantly different from that of a blank. Limit of detection was approved by calculations based on the standard deviation of the response (δ) and the slope (S) of the calibration curve at the levels approaching the limits according to equation LOD = 3.2 (δ/S). The LOD for CEA was 0.01 ng/mL.

Regeneration and Stability of the Biosensor. Regeneration of the admittance biosensor is a key factor for developing a practical biosensor. In this experiment, the regeneration of the proposed biosensor could be regenerated by simply immersing it in a stirred 0.1 M glycine−hydrochloric acid solution for 5 min and washed with water. A relative standard deviation (RSD %) of 3.6% was acquired when the electrode was repeated six times in consecutive measurements. The biosensor exhibited an acceptable stability with a 3.6% decrease of peak current to 50 ng/mL CEA in $Fe(CN)_6^{4-}/^{3-}$ (pH 5.9) at 0.5 mM H_2O_2 after 10 days storage at 4 °C. The good stability may be because protein molecules were attached firmly onto the surface of composite matrix.

Method Validation. The linearity, limit of detection, repeatability, reproducibility and robustness were the parameters used for the method validation. As mentioned before, the measuring range of the biosensor is linear in two concentrations ranges of CEA from 0.1 to 70 ng/mL and from 70 to 200 ng/mL with a detection limit of 0.01 ng/mL. Relative standard deviation percent (RSD%) of three replicate measurements (error bars in Figure 7) was calculated 4.1%. The sensitivity of the method was obtained 4.42 nC mL ng^{-1}.

The parameters of the repeatability and reproducibility were investigated to assess the precision of the technique. For the repeatability monitoring, three replicate standards samples of 10, 30, and 50 ng/mL were measured. Then, the mean concentrations were found to be 10.4, 31.5, 52.1 ng/mL and RSD% values of 3.8, 2.9, and 4.0%, respectively. Regarding the interday precision, the same three concentrations were measured for three consecutive days, the associated RSD% values of less than 4.6%.

For robustness of the method, a comparison was performed between the CEA assay results obtained by two analysts. The RSD% values performed in the same laboratory by the two analysts did not exceed 5.2%. On the other hand, the robustness was examined while the parameter values (pH of the eluent and the laboratory temperature) were being slightly changed.

Selectivity Study. Substances may interfere in CEA response including immunoglobulin, α-1-fetoprotein, L-cysteine, L-lysine, and L-glutamate (50 ng/mL) were investigated. Three test solutions, including (1) CEA standard solution (50 ng/mL), (2) standard solution of 50 ng/mL CEA containing the above interferences, and (3) a solution containing just the above interferences, were used. The obtained results showed that

RSD% of the biosensor response in presence of the interfering species is less than 4.4%.

Comparison with the Best Previously Reported CEA Electrochemical Biosensors. For comparison, the performances of the fabricated biosensor is compared with the previous reported CEA electrochemical biosensors based on utilization of different materials and methods as the working electrode (Table 1) and it was confirmed that the presented ZnO, Au nanoparticles based biosensor exhibited an excellent and reproducible sensitivity for CEA.

CONCLUSIONS

In conclusion, a novel signal amplified strategy used to develop an immunosensor for determination of CEA based on HRP/anti-CEA/AuNPs/ZnO NPs composite matrix modified Au electrode. Such nanocomposite matrix shows good properties for tunneling electrons between immobilized HRP and electrode surface and retaining the bioactivity of immobilized molecules. This immunoassay protocol had several attractive advantages including simple fabrication, long-time storage stability, high sensitivity, low detection limit and satisfactory recovery. To the best of our knowledge, this is the first report on using such a very high-sensitive and low detection limit technique as a detection method for CEA biosensor.

AUTHOR INFORMATION

Corresponding Author

*E-mail: norouzi@khayam.ut.ac.ir.

REFERENCES

(1) Gold, P.; Freedman, S. O. *J. Exp. Med.* **1965**, *121*, 439–462.
(2) Thomas, S. N.; Tong, Z.; Stebe, K. J.; Konstantopoulos, K. *Biorheology* **2009**, *46*, 207–25.
(3) Warsinke, A.; Benkert, A.; Scheller, F. W. *Fresenius' J. Anal. Chem.* **2000**, *366*, 622–34.
(4) Park, K. W.; Lee, W. H.; Choi, J. W. *Biosens. Bioelectron.* **2004**, *19*, 1497–1504.
(5) Penalva, J.; Puchades, R.; Maquieira, A. *Anal. Chem.* **1999**, *71*, 3862–72.
(6) Yu, H.; Yan, F.; Dai, Z.; Ju, H. X. *Anal. Biochem.* **2004**, *331*, 98–105.
(7) Aguilar, Z. P.; Vandaveer, W. R. I.; Frisch, I. *Anal. Chem.* **2002**, *74*, 3321–3329.
(8) Dai, Z.; Yan, F.; Chen, J.; Ju, H. X. *Anal. Chem.* **2003**, *75*, 5429–34.
(9) Darain, F.; Park, S. U.; Shim, Y. M. *Biosens. Bioelectron.* **2003**, *18*, 773–780.
(10) Norouzi, P.; Ganjali, M. R.; Shirvani-Arani, S.; Mohammad, A. *J. Pharm. Sci.* **2007**, 893–904.
(11) Norouzi, P.; Ganjali, M. R.; Zare, M.; Mohammadi, A. *J. Pharm. Sci.* **2007**, *96*, 2009–2017.
(12) Norouzi, P.; Ganjali, M. R.; Larijani, B.; Mirabi-Semnakolaii, A.; Mirnaghi, F. S.; Mohammadi, A. *Pharmazie* **2008**, *63*, 633–637.
(13) Norouzi, P.; Larijani, B.; Ezoddin, M.; Ganjali, M. R. *Mater. Sci. Eng., C* **2008b**, *28*, 87–93.
(14) Sole, S.; Alegret, S.; Cespedes, F.; Fabregas, E.; Diez-Caballero, T. *Anal. Chem.* **1998**, *70*, 1462–1467.
(15) Limbut, W.; Proespichaya, K.; Bo, M.; Punnee, A.; Panote, T. *Anal. Chim. Acta* **2006**, *561*, 55–61.
(16) Tang, H.; Jinhua, C.; Lihua, N.; Yafei, K.; Shouzhuo, Y. *Biosens. Bioelectron.* **2007**, *22*, 1061–1067.
(17) Dai, Z.; Feng, Y.; Hua, Y.; Xiaoya, H.; Huangxian, J. *J. Immunol. Method.* **2004**, *287*, 13–20.
(18) Ruo, Y.; Ying, Z.; Qin, C.; Ying, Z.; AiLi, S. *Sci. China, Ser. B: Chem* **2007**, *50*, 97–104.
(19) Liu, K. G.; Yuan, R.; Chai, Y. Q.; Tang, D. P.; An, H. Z. *Bioprocess Biosyst. Eng.* **2010**, *33*, 179–185.
(20) Liao, Y. H.; Yuan, R.; Chai, Y. Q.; Zhuo, Y.; Yang, X. *Anal. Biochem.* **2010**, *402*, 47–53.
(21) Li, J. P.; Gao, H. L.; Chen, Z. Q.; Wei, X. P.; Yang, C. F. *Anal. Chim. Acta* **2010**, *665*, 98–104.
(22) Laboria, N.; Fragoso, A.; Kemmner, W.; Latta, D.; Nilsson, O.; Botero, M. L.; Drese, K.; O'Sullivan, C. K. *Anal. Chem.* **2010**, *82*, 1712–1719.
(23) Zhuo, Y.; Yu, R. J.; Yuan, R.; Chai, Y. Q.; Hong, C. L. *J. Electroanal. Chem.* **2009**, *628*, 90–96.
(24) Zhang, T. T.; Yuan, R.; Chai, Y. Q.; Liu, K. G.; Ling, S. J. *Microchim. Acta* **2009**, *165*, 53–58.
(25) Viswanathan, S.; Rani, C.; Anand, A. V.; Ho, J. A. A. *Biosens. Bioelectron.* **2009**, *24*, 1984–1989.
(26) Guan, S.; Yuan, R.; Chai, Y. Q.; Tang, D. P.; Liu, K. G.; Wang, J. F. *Acta Chim. Sinica* **2009**, *67*, 1923–1928.
(27) Luo, X.; Xu, J.; Zhao, W.; Chen, H. *Biosens. Bioelectron.* **2004**, *19*, 1295–1300.
(28) Ahmad, M.; Pan, C.; Gan, L.; Nawaz, Z.; Zhu, J. *J. Phys. Chem. C* **2010**, *17*, 243–250.
(29) Tu, Y. Y.; Primus, F. J.; Shochat, D.; Goldenberg, D. M. *Tumor Biol* **1988**, *9*, 212–220.
(30) Casey, B. J.; Kofinas, P. *J. Biomed. Mater. Res. A* **2008**, *87A*, 359–363.
(31) Pingarrón, J. M.; Paloma, Y. S.; Araceli, G. C. *Electrochim. Acta* **2008**, *53*, 5848–5866.
(32) Daneshgar, P.; Norouzi, P.; Dousty, F.; Ganjali, M. R.; Moosavi-Movahedi, A. A. *Curr. Pharm. Anal.* **2009**, *5*, 246–255.
(33) Daneshgar, P.; Norouzi, P.; Ganjali, M. R. *Chem. Pharm. Bull.* **2009**, *57*, 117–121.
(34) Daneshgar, P.; Norouzi, P.; Ganjali, M. R. *Sens. Actuators B* **2009**, *136*, 66–72.
(35) Norouzi, P.; Qomi, M.; Nemati, A.; Ganjali, M. R. *Int. J. Electrochem. Sci.* **2009**, *4*, 1248–1261.
(36) Norouzi, P.; Rashedi, H.; Mirzaei Garakani, T.; Mirshafian, R.; Ganjali, M. R. *Int. J. Electrochem. Sci.* **2010**, *5*, 377–391.
(37) Norouzi, P.; Faridbod, F.; Nasli-Esfahani, E.; Larijani, B.; Ganjali, M. R. *Int. J. Electrochem. Sci.* **2010**, *5*, 1008–1017.